THE APPLICATION OF ITERATIVE EQUALISATION TO HIGH DATA RATE WIRELESS PERSONAL AREA NETWORKS

A. G. Lillie, A. R. Nix, P. N. Fletcher and J. P. McGeehan
University of Bristol, Centre for Communications Research, Merchant Venturers Building, Woodland Road, Bristol, BS8 1UB, UK

ABSTRACT

There is increasing demand for broadband wireless personal area networking devices, mainly fuelled by mobile multimedia applications such as wireless home networks. This paper investigates the suitability of iterative equalisation as a means of achieving low bit and packet error rates in a future high data rate personal area network standard. Baseband simulation results demonstrate the powerful ISI mitigation and error correcting performance of such receivers when operating in representative indoor wideband channels.

INTRODUCTION

Wireless Personal Area Network (WPAN) communication systems allow electronic devices in close proximity to each other to network and communicate without the need for wired connections. The range of applications that these systems support can be divided into three broad areas; mobile, covering devices such as phones and cameras, stationary, encompassing desktop computing and its associated peripherals and consumer electronics, incorporating home appliances such as televisions and videos [1]. One key advantage of a WPAN is the manner in which ad hoc connections can be easily and transparently established between a number of heterogeneous devices.

Bluetooth is an emerging standard for WPAN communication based on a low cost, low power, worldwide operation ethos [2]. An increased number of products supporting many varied consumer electronic applications are expected to emerge into the market place in the next few years with unit sales predicted in the hundreds of millions. The Bluetooth radio interface has a raw data rate of 1Mb/s, giving a unidirectional maximum user data rate of 725 kb/s, which is sufficient for the majority of non-time bounded applications [3]. However, for applications such as mobile multimedia, home servers and TV/VCR video distribution, raw data rates in excess of 10Mb/s are required. To facilitate these rates, a high data rate personal area network standard is required.

In order to achieve data rates that meet the requirements of these applications, a number of strategies can be employed. The symbol rate and therefore the operating bandwidth can be substantially increased. This can also be combined with the use of M-ary modulation techniques in an adaptive modulation solution. However, the proposed increase in bandwidth and modulation level makes the resulting transmissions more susceptible to delay dispersion in the radio channel. This manifests as increased inter symbol interference (ISI) at the receiver. ISI in turn results in an irreducible bit error rate (BER) and packet error rate (PER) floor, which for applications such as home video distribution is unacceptable.

Since the initial proposal of 'Turbo Codes' by Berrou et al in 1993 [4], the iterative principle has been extended to encompass single carrier equalisation techniques. This allows single carrier systems to combine the operations of equalisation and channel coding to operate in a wideband channel with performance that could not previously be achieved with traditional equalisation and forward error correcting (FEC) techniques [5]. Iterative equalisation techniques have been shown to give excellent error rate performance for both fixed and fast fading channels [6].

This paper investigates the suitability of including iterative equalisation in the receiver to combat ISI. BER and PER results are presented for BPSK, QPSK and 8-PSK modulation schemes in a number of slow Rayleigh fading channel scenarios which are representative of indoor channel conditions. The channel models are characterised in terms of normalised delay spread, which allows comparison independent of system symbol rate. Through the use of a simple link budget and rate calculations, predicted data rate versus, both signal to noise ratio (SNR) and range are presented. This gives an indication of the expected performance for each of the channels.

The paper concludes by determining under what channel conditions and modulation modes it is appropriate to use multiple iterations of a Maximum A-Posterior (MAP) equaliser/decoder pair at the receiver to mitigate the effect of ISI. For certain channel conditions, one iteration is sufficient to mitigate ISI and is often optimal. Following this, the complexity of the receiver is analysed and techniques for its reduction are discussed. Finally conclusions are drawn about the suitability of including iterative equalisation for use in WLAN solutions.

BASEBAND SIMULATION STRUCTURE

For the purpose of this study, the baseband simulation shown in Figure 1 has been developed.

ENCODING

The payload element of a packet is made up of 500 data bits, which are encoded with the half rate recursive systematic convolutional (RSC) encoder shown in Figure 2, to form a data block of 1004 bits. The final 4 bits are appended to ensure that the encoder is returned to the zero state at the end of the block. This is achieved by switching off the input bit stream and considering only the feedback bits as the input to the encoder [7].

Manuscript received June 24, 2002

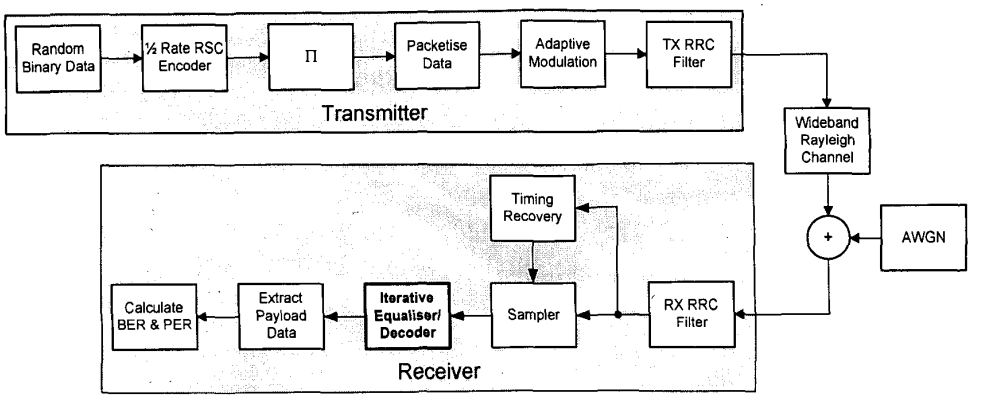

Figure 1, Baseband Structure

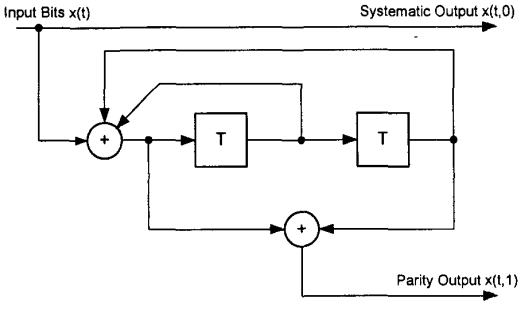

Figure 2, Half Rate Recursive Systematic Convolutional Encoder

The RSC encoder can be described by the generator polynomial given in (1). This encoder is of input constraint length CL=2 and therefore produces a trellis structure with $2^{CL} = 4$ states.

$$G = \left[1, \frac{101}{111}\right] \begin{matrix} Output \\ Feedback \end{matrix} \qquad (1)$$

Figure 3, shows the bit error rate (BER) versus signal to noise ratio (SNR) performance for this code using BPSK, QPSK and 8-PSK modulation, transmitted over an Additive White Gaussian Noise (AWGN) channel and decoded with the MAP algorithm [8]. These performance curves are important, as they represent an upper bound on performance for the iterative equalisation receivers which follow in this study [6]. When the respective bound is met, this indicates complete mitigation of inter-symbol interference (ISI) introduced by the wideband channel.

INTERLEAVING

The encoded data block is then passed through a random interleaver of size 1004 elements, denoted in Figure 1, by the Π symbol. This is necessary to allow iterative equalisation at the receiver. The interleaver ensures de-correlation between the data block and the symbols that are passed through the channel.

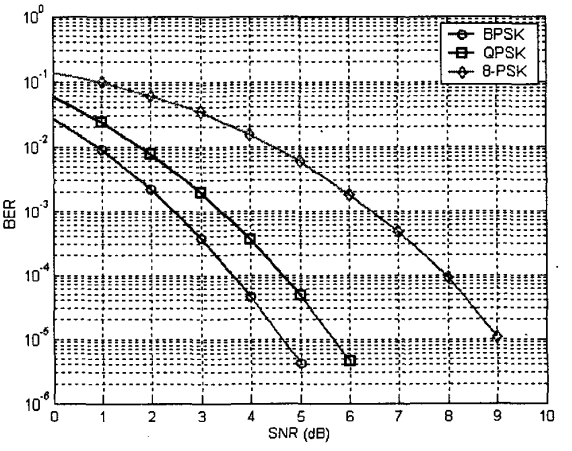

Figure 3, Performance of MAP Decoding on Half Rate RSC Code

PACKET STRUCTURE

The payload is formed into a packet following the structure shown in Figure 4. A 100 bit training sequence is attached to the start of the packet, to allow for channel estimation with the LMS algorithm [9]. Simulation has shown that this is of adequate size to allow convergence for the channel lengths used in this study. Also included is a 100 bit header which would contain information such as the modulation mode for the payload block which follows, here it contains random bits. Pre- and Post-amble's consisting of zero symbols are also attached to the payload each of length M symbols, where M is the channel memory order, to ensure that the channel begins and ends in the zero state. This is necessary for iterative equalisation.

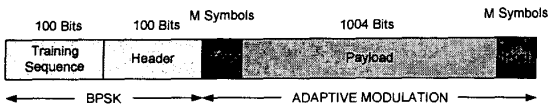

Figure 4, Packet Structure

Once formed, the packet is modulated, with the training scheme and header always using BPSK modulation and the payload using BPSK, QPSK or 8-PSK modulation as shown in Figure 4. The modulated packet size is therefore variable, but contains a fixed amount of information bits. The interleaver size, which is dependent on the number of information bits and the code rate and is a performance factor in the iterative receiver, is therefore fixed.

TRANSMIT FILTERING

Prior to transmission the modulated data is filtered with a root raised cosine (RRC) filter with a roll-off factor $\alpha = 0.4$ and a span of 11 symbols. Up-sampling is performed in the filter to a rate of 8 samples per symbol, so the filter contains 89 taps.

CHANNEL MODEL

A mobile radio channel with inter-symbol interference (ISI) can be described by a tapped delay line structure as shown in Figure 5 [10]. The tap coefficients $h(T_s)$ are time-varying complex values related to the operating environment propagation conditions, where T_S is the sampling period of the system.

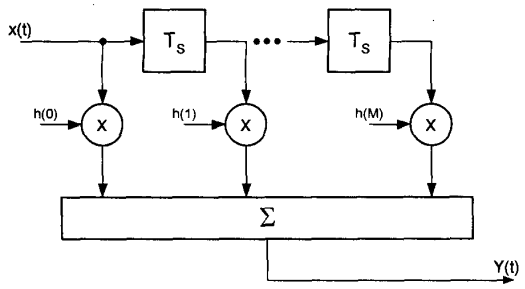

Figure 5, Wideband Channel Model

For indoor propagation environments, these tap coefficients can be described by the equation:

$$h(\tau) = \sum_{k=0}^{M} \alpha_k(t) e^{-j\theta_k(t)} \delta(\tau - \tau_k(t)) \qquad (2)$$

where α_k , θ_k and τ_k are the attenuation, phase and delay associated with the k^{th} component. By assuming that the statistics of the channel can be described as wide-sense stationary uncorrelated scattering then each of the coefficients is subject to complex Gaussian fading, ie Rayleigh fading. If the maximum velocity of motion of objects within the indoor environment is 5m/s, then for a system operating in the 2.4GHz band, the Doppler frequency will not exceed 40Hz. It is therefore reasonable to assume that over the packet transmission time the channel conditions will be static. The channel is described as 'Slow Rayleigh Fading'.

For the purpose of this study, the average impulse response of the channel will be exponentially decaying and can be characterised by its root mean square (RMS) delay spread τ_{RMS}, given by:

$$\tau_{RMS} = \left[\frac{\sum_{k=0}^{M} (\tau_k - \tau_a)^2 \sigma_k}{\sum_{k=0}^{M} \sigma_k} \right] \text{where } \tau_a = \frac{\sum_{k=0}^{M} \tau_k \sigma_k}{\sum_{k=0}^{M} \sigma_k} \qquad (3)$$

where σ_k represents the received power after a delay of τ_k seconds and τ_a represents the centroid of the power delay profile. The delay spread is normalised to the symbol transmission rate R_S so that the normalised delay D is given by:

$$D = \tau_{RMS} \times R_S \qquad (4)$$

The purpose of this is to allow general system comparison without specifying the symbol rate. It has been shown that it is possible to generate an impulse response with a given RMS delay spread using equation 5 [11]. By substituting (4) in to (5) an impulse response with a given normalised delay spread can be generated, as shown in equation 6, where υ is the number of samples per symbol.

$$h(k) = \exp\left[\sqrt{\frac{-kT_s}{\tau_{RMS}}} \right] \qquad (5)$$

$$h(k) = \exp\left[\sqrt{\frac{-k}{\upsilon \times D}} \right] \qquad (6)$$

The maximum delay spread of the channel, is limited to four times the symbol period of the systems and is therefore limited to four times the normalised delay spread. Figure 6, shows the power delay profile for a channel with normalised delay spread D=0.5.

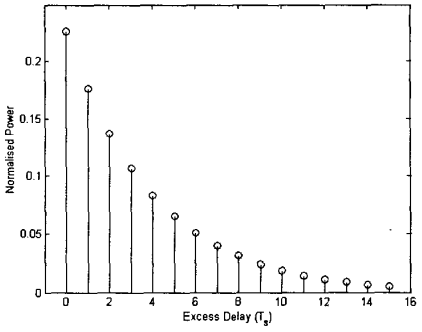

Figure 6, Channel A, Power Delay Profile

If the symbol rate is assumed to be 10MHz, then the wanted RMS delay spread τ_{RMS} = 50nS. The measured RMS delay spread of the power delay profile assuming a symbol rate of 10MHz is 48.94nS. In order to evaluate the receiver structure a number of channels are defined, having properties summarised by Table 1.

Channel Model	Normalised Delay Spread (D)	Symbol Span	Number of T_s Spaced Taps
A	0.5	2	16
B	1	4	32
C	2	8	64

Table 1, Channel Model Specifications

RECEIVE FILTERING AND TIMING RECOVERY

At the receiver, the received data stream is filtered using an identical RRC filter to the one used at the transmitter. In this study, ideal symbol and sample timing point recovery is used.

ITERATIVE EQUALISATION

Figure 7, shows the iterative equalisation receiver structure used in this study. Both the equaliser and the decoder employ the optimal symbol by symbol Maximum A-Posteriori (MAP) soft input soft output (SISO) algorithm [12]. Soft input symbols are fed into the decoder from a sampled receive filter stream *r(t)* and bit-wise hard decisions are produced as the final output.

The RSC encoder and the channel can be considered as a serially concatenated coding scheme, similar to that of a serially concatenated turbo encoder [13]. This observation means that it is possible to replace the first MAP decoder in a serial turbo receiver with a MAP equaliser. It is possible to equalise and decode in an iterative manner that is similar to turbo decoding.

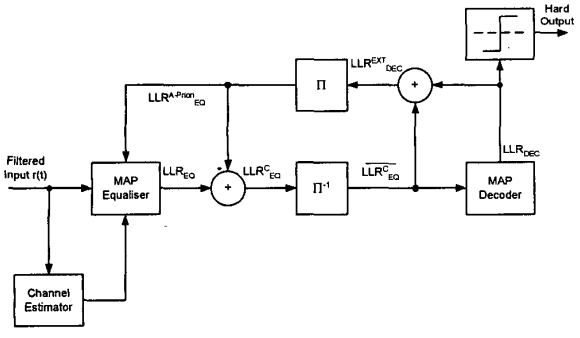

Figure 7, Iterative Equaliser Structure

The MAP equaliser accepts received channel symbols *r(t)* and a-priori information about the encoded bits $LLR_{EQ}^{A\text{-}Priori}$ as well as a channel estimate. It produces Log Likelihood Ratio (LLR) values about the original encoded bits at the output LLR_{EQ}. On the first iteration, the a-priori information at the input to the equaliser is initialised to zero. On subsequent iterations, it is derived from the output of the MAP decoder.

$$LLR_{EQ}^{C} = LLR_{EQ} - LLR_{EQ}^{A\text{-}Priori} \tag{7}$$

By subtracting (7) the a-priori information from the LLR output of the equaliser, soft estimates of the encoded bits $\overline{LLR_{EQ}^{C}}$ can be fed into the MAP decoder after de-interleaving. The MAP decoder produces LLR values about both the information bits and the parity bits. This is a modification compared to a MAP decoder used in turbo [6]. The equaliser requires a-priori information about all bits, which are derived from this output. This a-priori information is calculated by first subtracting the LLR input to the decoder $\overline{LLR_{EQ}^{C}}$ from its output (8) and then interleaving. Hard decisions can be made after any number of iterations, by considering the sign of the information bit LLR output of the decoder.

$$LLR_{DEC}^{EXT} = LLR_{DEC} - \overline{LLR_{EQ}^{C}} \tag{8}$$

MAP ALGORITHM FOR EQUALISATION AND DECODING

A general MAP module, that can either function as a decoder or an equaliser has inputs and outputs as shown in Figure 8. The module accepts Log Likelihood Ratio (LLR)(9) values y about the received sequence as well as LLR a-priori values P(x) for the received bits. These may be obtained from prior knowledge of the original data or from a previous decoding stage.

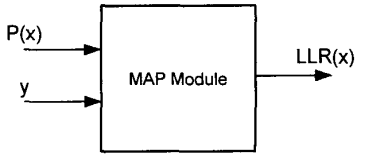

Figure 8, General MAP module

$$LLR(x) = \log\left[\frac{p(x=+1)}{p(x=-1)}\right] \tag{9}$$

The output of a MAP module is given as a LLR which can be calculated as:

$$LLR(x) = \log\left[\frac{p(x=+1|y)}{p(x=-1|y)}\right] = \log\left[\frac{\sum_{(s',s)x=+1} p(s',s,y)}{\sum_{(s',s)x=-1} p(s',s,y)}\right] \tag{10}$$

Where *s'* denotes the current state at level *k*-1 and *s* the next state at level *k* of the trellis and *y* the input LLR. The joint probability p(s',s,y) can be expressed as a product of three separate probability terms:

$$p(s',s,y) = p(s',y_{j<k}) \times \left[p(s|s')p(y_k|s',s)\right] \times p(y_{j>k}|s) \quad (11)$$
$$= \alpha_{k-1}(s') \times \gamma_{k-1}(s',s) \times \beta_k(s)$$

These are diagrammatically shown in Figure 2. Through forwards recursion α can be calculated using (12) and using a backwards recursion β is calculated using (13) [14].

$$\alpha_k(s) = \frac{\sum_{s'} \alpha_{k-1}(s') \times \gamma_k(s',s)}{\sum_s \sum_{s'} \alpha_{k-1}(s') \times \gamma_k(s',s)} \quad (12)$$

$$\beta_{k-1}(s') = \frac{\sum_s \beta_k(s) \times \gamma_k(s',s)}{\sum_s \sum_{s'} \alpha_{k-1}(s') \times \gamma_k(s',s)} \quad (13)$$

In order to calculate the α and β terms, the trellis must be of finite duration. Decoding is performed on a block basis. It is therefore assumed that the trellis begins and ends in the zeros state, under this assumption we can initialise α and β as follows:

$$\alpha_0(0) = 1, \alpha_0(\neq 0) = 0$$
$$\beta_{end}(0) = 1, \beta_{end}(\neq 0) = 0 \quad (14)$$

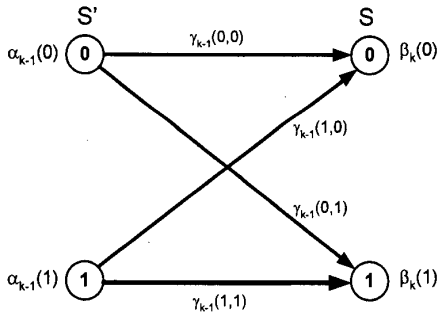

Figure 9, Trellis Structure

For transitions that exist, the branch transition probability $\gamma_k(s',s)$, can be expressed as product of the transition probability and the a-priori probability:

$$\gamma_k(s',s) = p(y_k|s',s) \times P(x_k) \quad (15)$$

Up to this point, the MAP module has been general, in that there is nothing to differentiate between an equaliser and a decoder. The difference lies in the calculation of the branch transition probability $\gamma_k(s',s)$.

MAP EQUALISER

A MAP Equaliser accepts at its inputs, complex valued received symbols r_ε at time ε, as well as, complex valued symbol spaced channel coefficients $g_i(t)$ from the M memory discrete time channel model. It also accepts a-priori information from a previous decoding stage P(x). For transitions that exist, the branch transition probability corresponding to a transition caused by x_ε is calculated by [6]:

$$\gamma_\varepsilon(s',s) = \exp\left(\frac{1}{2} \times x_\varepsilon \times P(x_\varepsilon)\right) \times \gamma_\varepsilon^{Ext}(s',s)$$
$$= \exp\left(\frac{1}{2} \times x_\varepsilon \times P(x_\varepsilon)\right) \times \exp\left[-\frac{1}{2\sigma^2}\left|r_\varepsilon - \sum_{i=0}^{M} g_i(t) \times x_{\varepsilon-i}\right|^2\right] \quad (16)$$

where σ^2 is the noise variance. Due to the non-systematic, non-binary nature of the channel, it is not possible to separate at the output of the equaliser the extrinsic and channel LLR values, given in the second term of (16). The output of the equaliser can therefore be expressed as a sum of two terms:

$$LLR(x) = P(x) + \log\left[\frac{\sum_{(s',s)x_\varepsilon=+1} \gamma_\varepsilon^{Ext}(s',s) \times \alpha_{\varepsilon-1}(s') \times \beta_\varepsilon(s)}{\sum_{(s',s)x_\varepsilon=-1} \gamma_\varepsilon^{Ext}(s',s) \times \alpha_{\varepsilon-1}(s') \times \beta_\varepsilon(s)}\right] \quad (17)$$

It is for this reason that it is not possible to supply the COD-MAP decoder with separate a-priori information which would have stemmed from the extrinsic output of the equaliser.

COD-MAP DECODER

The COD-MAP decoder, accepts at its input, LLR's about both the systematic and parity bits from the coded data stream $L(x_{k,v})$. Using these it produces LLR values at its output for both the systematic and parity bits which are required by the MAP equaliser. There is no a-priori input, as it is assumed that in the original data bits, P(+1)=P(-1)=0.5 and no separate a-priori information can be obtained from the output of the equaliser. The branch transition probability is therefore given as:

$$\gamma_k(s',s) = \exp\left(\sum_{v=0}^{N-1}\left(\frac{1}{2} \times L(x_{k,v}) \times x_{k,v}\right)\right) \quad (18)$$

where N is the inverse of the code rate, i.e. in a ½ rate coded system there is one systematic bit $x_{k,0}$ and one parity bit $x_{k,1}$. Due to the systematic, binary nature of the encoder, it is possible to separate the extrinsic and received LLR values at the output of the decoder. The LLR output in this ½ rate system is given as:

$$LLR(x_{k,v}) = L(x_{k,v}) + \log\left[\frac{\sum_{(s',s)x_{k,u\neq v}=+1} \exp\left(\frac{1}{2} \times L(x_{k,u\neq v}) \times x_{k,u\neq v}\right) \times \alpha_{\varepsilon-1}(s') \times \beta_\varepsilon(s)}{\sum_{(s',s)x_{k,u\neq v}=-1} \exp\left(\frac{1}{2} \times L(x_{k,u\neq v}) \times x_{k,u\neq v}\right) \times \alpha_{\varepsilon-1}(s') \times \beta_\varepsilon(s)}\right] \quad (19)$$

BER AND PER PERFORMANCE

The BER and PER performance of an iterative equaliser is dependent upon the channel profile, the modulation scheme, the encoder constraint length and also the size of the interleaver. In this study, the encoder constraint length and the size of the interleaver are fixed. The results that follow demonstrate the effect of changing the channel delay spread with a fixed modulation scheme and secondly, for a fixed delay spread increasing the modulation order.

Figures 10a and 10b show the BER and PER performance versus average SNR respectively, when BPSK modulation is used with each of the three channel models. From Figure 10a, we note two separate trends as the channel changes, corresponding to an increase in the normalised delay spread. For a target BER rate of $1*10^{-3}$, it can be seen that on the 3rd iteration a gain of approximately 2.2dB is seen for channel B compared to channel A. This corresponds to a change in normalised delay spread from 0.5 to 1.0. A gain of similar magnitude is experienced as the delay spread increases to 2.0 for channel C. This gain can be attributed to the increased memory length of the channel. The second trend, sees the iterative gain increase as the normalised delay spread increases. If we take the same BER target, we see that the gain for channel A between iteration 1 and 2 is negligible. For channel B, the gain is noticeable, being approximately 0.5dB. This rises again, for channel C to 0.7dB. In all cases, there is no iterative gain beyond the second iteration. When we examine Figure 10b, the PER versus SNR performance, we note the same trend, with larger iterative gains. At a target PER of 1%, we see a gain of 1.1dB for channel C. Figure 10a, also shows the AWGN bound, corresponding to the upper limit of performance for BPSK modulation. At the target BER, for channel C, there is a degradation of 5.5dB from the bound. This degradation can be attributed to two main factors. Figure 11a, shows the BER performance for BPSK on a static channel assuming the average profile of Channel B. It shows that at the target error rate we suffer approximately 0.8dB degradation from the AWGN bound after 5 iterations. Imperfect channel state information (CSI) is the main cause of this. If perfect CSI is known at the receiver, then we see from Figure 11b that the degradation is now only 0.1dB after 5 iterations. The performance bound is met above 4dB, indicating the complete mitigation of ISI. The second, more significant contributing factor to the degradation is the effect of 'Slow Rayleigh Fading' on the error distribution as shown in Figure 12. These error distributions, for iterations 1 to 3 show two things. Firstly, we see that there is a high frequency of packets with very few errors occurring after iteration 1. 72% of the packets have no errors and 90% of the packets have less than 20 errors. By iteration 3, this has risen to 80% with no errors and 95% with less than 20 errors. The iterative equaliser is performing very well for the majority of channels. However, there are a small number of packets, which the iterative equaliser has failed to equalise/decode, after iteration three, 1% have more than 100 errors. These packets will dominate the BER results. This occurs, when the dominant taps at the start of the channel profile are subject to deep fading. The received power at this point drops to such a level, that the equaliser sees a signal with very low instantaneous SNR making it impossible to equalise with any certainty. On subsequent iterations, the a-priori information may even raise the uncertainty because the soft feedback is incorrect, leading to an increased number of bit errors.

Figure 13, shows the BER and PER performance for BPSK, QPSK and 8-PSK modulation when transmitted over channel model B. If again we take the target BER as $1*10^{-3}$, then to achieve this target, the BPSK mode requires 10dB SNR, QPSK 16dB and 8-PSK 23dB. With increasing modulation order, the degradation with respect to the relevant bound increases. For the BPSK mode a degradation of 7.9dB is experienced, QPSK and 8-PSK suffer 12.7dB and 16.5dB respectively. As the modulation order increases a third trend is apparent, the iterative gain increases. At the target error rate, the gain from iteration 1 to 2 for BPSK is 0.5dB, for QPSK 1dB and the projected gain for 8-PSK is 3.2dB. As before, there is very little gain associated with further iterations greater than the second.

DATA RATE ANALYSIS

The instantaneous data rate DR against SNR_{dB} can be calculated from the packet error rate as follows:

$$DR_{SNR} = (R_S \times K) \times \left(\frac{k}{n}\right) \times \left(1 - PER_{SNR}\right) \qquad (20)$$

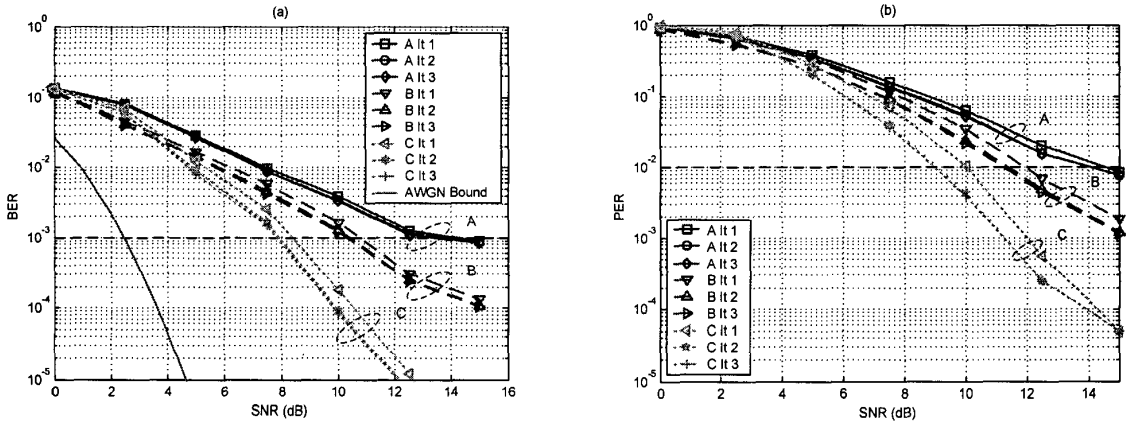

Figure 10, a. BER and b. PER for Channels A, B and C using BPSK Modulation

where K is the bandwidth efficiency, k is the number of information bits and n is the total number of bits per packet, i.e. (k/n) is the packet code rate. It is assumed that no packets are discarded due to header errors. The PER and therefore T is purely a function of the payload error rate. This quantative measure allows us to compare each of the modulation modes and channel scenarios presented earlier in terms of the expected achievable data rates versus SNR.

$$SNR_{dB} = P_R - N \tag{21}$$

In order to examine the achievable data rates versus range, a link budget must be established [15, 16]. To calculate the SNR, given by (21) at the receiver, we must consider expressions for the noise power N and also the receiver power P_R in terms of the transmit power P_T and the path loss P_L:

$$N = 10\log_{10}(K_B T) + 10\log_{10}(R_S \times (1+\alpha)) + NF \tag{22}$$

where K_B = 1.38e-20 mW/Hz/Kelvin, T=300 Kelvin and NF is the receiver noise figure and:

$$P_R = P_T + P_L$$
$$P_L = G_T + G_R + 20\log_{10}\left(\frac{\lambda}{4\pi}\right) - n\times 10\log_{10}(d) \tag{23}$$

where G_T and G_R are the gains of the transmit and receiver antennas respectively relative to an isotropic source, λ is the wavelength of the carrier frequency and d the separation between the antennas. n is an empirical constant, the path loss exponent, which for line of sight (LOS) is 2 and greater than 2 for non-LOS conditions. We assume a path loss exponent of 4, which represents a worst case scenario, an indoor environment with high clutter.

In order to perform a meaningful comparison, the symbol rate must be known. Figure 14, shows the RMS delay spread versus symbol rate for varying normalised delay spreads. If a nominal symbol rate of 20MHz is selected, then the RMS delay spread for channel models A,B and C is 25ns, 50ns and 100ns respectively. In an indoor environment, RMS delay spreads of up to 50ns will be commonly encountered. WPANs may also be expected to operate in an indoor to outdoor scenario where RMS delay spreads reaching 100ns or greater may be encountered. These RMS delay spread are therefore representative of the type of conditions that may be encountered in a real operating environment.

The maximum actual data rates achievable for the different modulation modes are shown in Table 2 calculated from (20) assuming a symbol rate of 20MHz and the packet structure already described. Because of the small payload size and the half rate code, the percentage user data is only 41.5% of the total transmitted data.

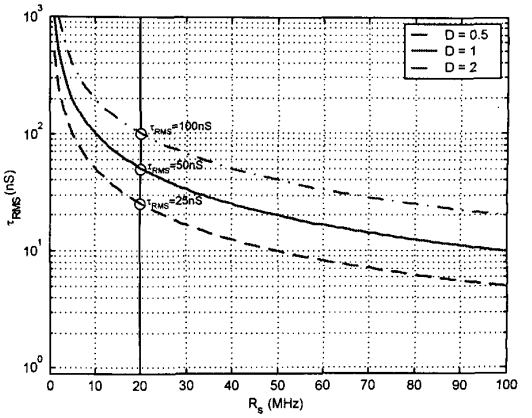

Figure 14, RMS Delay Spread vs. Symbol Rate for Fixed Normalised Delay Spread

Mode	Rate (MHz)
BPSK	8.3
QPSK	16.6
8-PSK	24.9

Table 2, Maximum Achievable Data Rates

The transmission parameters given in Table 3 are assumed in the link budget analysis.

Figures 15 and 16 show the data rate versus SNR and range for all three channel models using BPSK modulation and BPSK, QPSK and 8-PSK modulation using channel model B respectively.

Parameter	Value
Rs	20 MHz
α	0.4
N_F	10 dB
P_T	0 dBm
G_T	0 dB
G_R	0 dB
f_C	2.4 GHz
λ	0.125 m
n	4

Table 3, Transmission Parameters

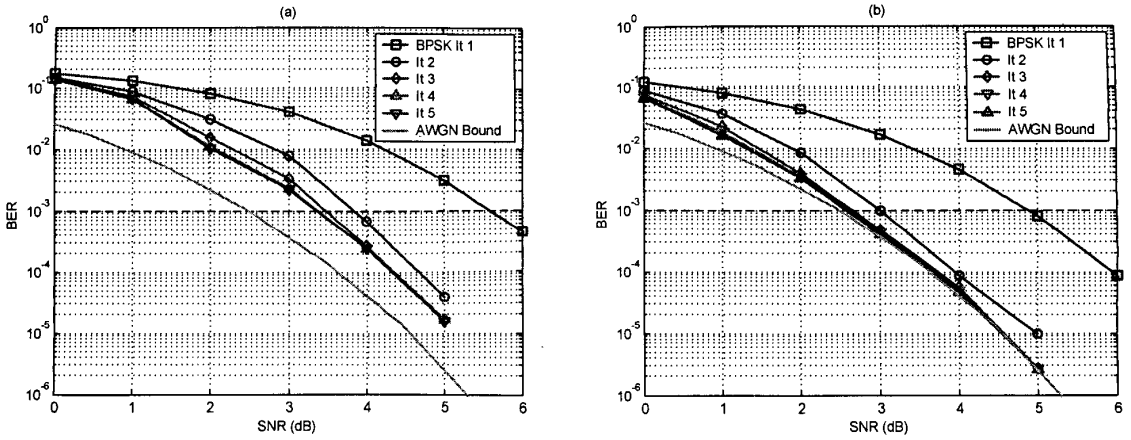

Figure 11, BER for BPSK Modulation and Static Channel B, a. LMS CSI, b. Perfect CSI

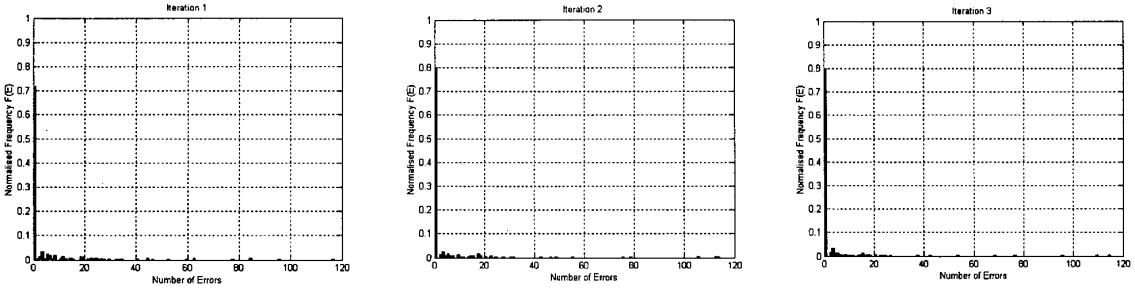

Figure 12, Error Distribution for Channel C at SNR 5.0dB

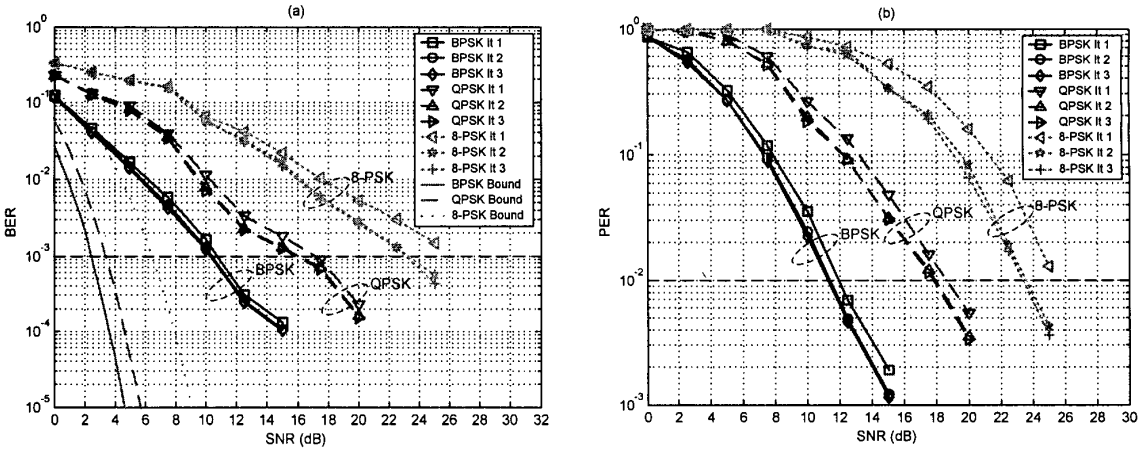

Figure 13, a. BER and b. PER for Channel B using BPSK, QPSK and 8-PSK Modulation

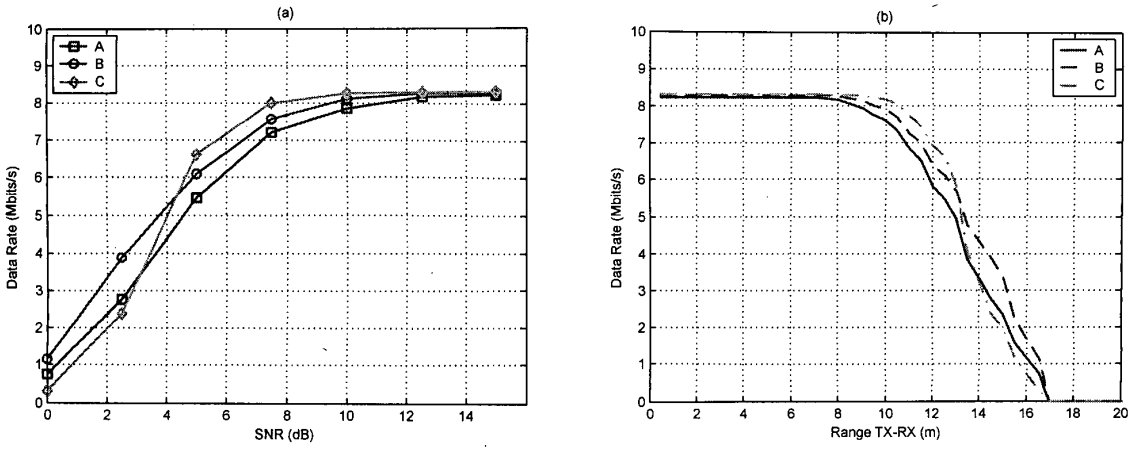

Figure 15, a. Data Rate vs. SNR and b. Data Rate vs. Range using BPSK Modulation for Channels A, B and C

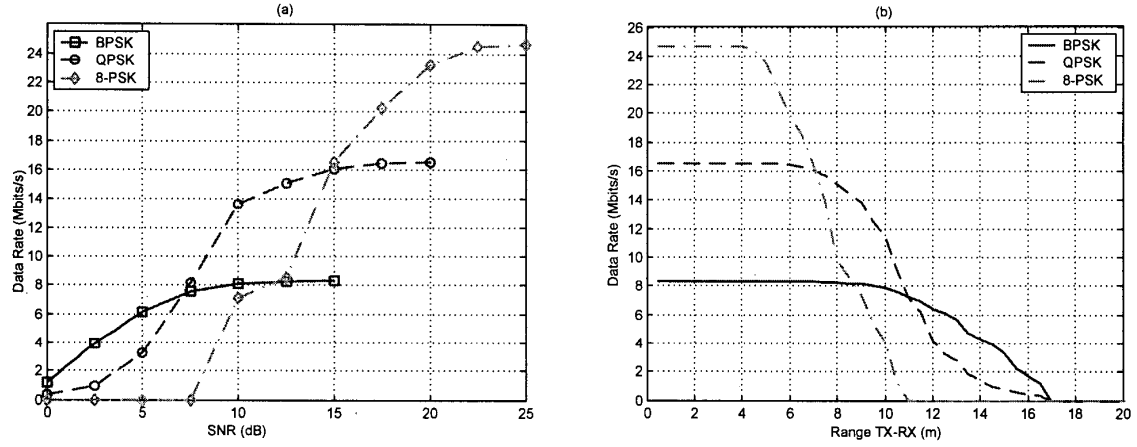

Figure 16, a. Data Rate vs. SNR and b. Data Rate vs. Range for Channel B using BPSK, QPSK and 8-PSK Modulation

Figure 15a, shows that at 4dB SNR using the BPSK mode, a user data rate of approximately 5Mbits/s is achieved for all channel conditions. Above this SNR, Channel C, with the largest delay spread, achieves the highest data rate until all modes reach the maximum rate at around 14dB SNR. The data rate versus range graph, Figure 15b, shows that for all channel conditions, at a range less than 13m, an instantaneous data rate greater than 5Mbits/s should be achieved.

Figure 16a shows that if BPSK, QPSK and 8-PSK modes were all used in an adaptive modulation scheme then over a SNR ratio range of 0 to 25dB, all three modes would be used to maximise the instantaneous data rate. Below 7.5dB, the BPSK mode produces the greatest rate, reaching a maximum of 7.8Mbits/s before the QPSK mode is used up to 15dB where it has a maximum rate of 16Mbits/s. Above this SNR 8-PSK is used, reaching a maximum rate of 24.9Mbits/s at 23dB. Figure 16b, indicates that at ranges less than 6m, the 8-PSK mode will deliver data rates greater than 20Mbits/s.

CONCLUSION

The results presented for BPSK modulation over all three channels show that the BER and PER performance improves as the delay spread in the channel increases. They also show that for BPSK, one iteration is optimal for a channel with a delay spread of 0.5. For normalised delays greater than 1, there is a measurable benefit in employing a second iteration.

The results for higher modulation schemes show that as the modulation order increases, a higher SNR is required to obtain the same BER and PER performance as a lower order. They also demonstrate that the iterative gain is greater for higher modulation orders. However, there is a trade off, between the iterative gain for higher modulation orders and the complexity of the receiver. The complexity at the receiver is dominated by the complexity of the MAP equaliser. The number of states in the equaliser trellis is dependent upon both the modulation order and

the memory of the channel. In the decoder the trellis size is only dependent on the constraint length L of the code.

There are a number of different approaches to describing the complexity of the MAP algorithm [8, 17, 18]. Using the technique described in [18] the relative complexity of the MAP equaliser for each modulation mode and channel, relative to the complexity of a MAP decoder operating on a ½ rate code of constraint length 1, is given in table 4. The complexity calculations assume that the algorithms are full complexity and are based upon the equations presented here. The calculations are per output bit and take no account of memory requirements.

Modulation Order	Channel A (2 Tap)	B (4 Tap)	C (8 Tap)
2	1	4	64
4	9	144	36981
8	98	6290	257650010

Table 4, MAP Equalisation Complexity Relative to a ½ Rate MAP Decoder

When receiver complexity is considered, then it is apparent that it is infeasible to use this type of iterative equalisation technique with high modulation orders combined with channels with large delay spreads due to the huge relative complexity. There are techniques that allow iterative equalisation using filter based approaches that are independent of modulation order in their complexity [19]. This is particularly attractive for higher modulation orders. Future work will see their comparison with the MAP based approach presented here.

Using the nominal symbol rate of 20MHz, the RMS delay spreads are quantified as 25, 50 and 100ns for channel models A, B and C respectively. Using these, results are presented showing achievable data rates versus SNR. Theses indicate that BPSK, QPSK and 8-PSK modulation modes could be combined effectively in an adaptive modulation scheme where the normalised delay spread is 1. For the BSPK mode, results show that it is possible to achieve a data rate greater than 5Mbits/s for channels with less than 100ns RMS delay for a SNR greater than 4.4dB.

Data rate versus range calculations give an indication that it should be possible to maintain a data rate greater than 5Mbits/s using the BPSK mode for RMS delay spreads less than 100ns up to a range of 13m. Using adaptive modulation for a channel with 50ns RMS delay spread, rates between 12 and 24 Mbits/s may be obtained to a range of 10m. These results are a worst case analysis. If the WPAN was operating in an indoor to outdoor environment, perhaps as access to a fixed public network, then the path loss exponent may be as low as 2. This would increase the range to the order of 100m. Further work in this area, will see the integration of these results with a state of the art Ray Tracing propagation tool to give a better indication of data rates in scenario driven environments [19, 3].

The results presented here show iterative MAP equalisation is attractive in a WPAN system only when the modulation order is low due to receiver complexity, even though the iterative gains are greater for higher modulation orders. They also show that at low delay spreads, one iteration will be optimal i.e. a soft equaliser followed by a soft decoder. At higher RMS delay spreads, a second iteration will be of benefit.

ACKNOWLEDGMENTS

A.G. Lillie would like to acknowledge the financial support of the Engineering and Physical Sciences Research Council (EPSRC) and the financial and academic support of Toshiba Research Europe Limited (TREL).

REFERENCES

1. The Complete Guide to Bluetooth from Toshiba, ©Toshiba Information Systems (UK) Ltd, 2000
2. The Bluetooth Standard Version 1.0b http://www.bluetooth.com
3. A.K. Arumugam, S.M.D. Armour, B.S. Lee, M.F.Tariq and A.R. Nix, "Consumer electronics application and coverage constraints using Bluetooth and proposed Bluetooth evolution technologies", *IEEE Transactions on Consumer Electronics*, Vol.47, No. 3, 2001
4. C. Berrou, A. Glavieux and P. Thitimajshima, "Near Shannon limit error-correcting coding: Turbo Codes", *Proceedings IEEE International Conference on Communications*, 1993
5. C. Douillard, M.Jezequel, C. Berrou, A. Picart, P. Didier and A. Glavieux, "Iterative correction of intersymbol interference: Turbo-equalization", *European Transactions on Telecommunications*, vol. 6, pp. 507-511, September 1995
6. G. Bauch, H. Khorram and J. Hagenauer, "Iterative equalisation and decoding in mobile communication Systems", *Second European Personal Mobile Communications Conference (EPMCC)*, 1997
7. P. Sweeney, Error Control Coding an Introduction, Prentice Hall, 1991
8. B. Vucetic and J. Yuan, Turbo codes principles and applications, Kluwer Academic Publishers, 2000
9. S. Haykin, Adaptive Filter Theory, Prentice Hall, 1996
10. J.D. Parsons, The Mobile Propagation Channel, Wiley, 1992
11. Y. Sun, A rigorous physical layer investigation of next generation high performance radio LANs, , PhD Thesis, University of Bristol, 1997
12. L. Bahl, J. Cocke, F. Jelinek and J. Raviv, "Optimal decoding of linear codes for minimising symbol error rate", *IEEE Transactions on Information Theory*, Vol IT-42, pp 425-429, March 1996
13. S. Benedetto, D. Divsalar, G. Montorsiand F. Pollara, "Serial concatenation of interleaved codes: performance analysis,design, and iterative decoding" *IEEE Transactions on Information theory*, vol. 44, no. 3, may 1998
14. W.E. Ryan, "A turbo code tutorial", Unpublished
15. J.G. Proakis, Digital Communications, McGraw Hill 1989
16. Application of Digital Wireless Technologies to Global Wireless Communications, Seiichi Sampei, Prentice Hall, 1997
17. A.J. Viterbi, "An intuitive justification and a simplified implementation of the MAP decoder for convolutional codes" *IEEE Journal on Selected Areas in Communications*, Vol. 16, No. 2 Feb. 1998

18. P.H-Y. Wu, "On the complexity of turbo decoding algorithms", *Proceeding IEEE Vehicular Technology Conference*, Spring 2001
19. C. Laot, A. Glavieux, J. Labat, "Turbo equalization: Adaptive equalization and channel decoding jointly optimized", *Journal on Selected Areas in Comunications*, Vol. 19, No. 9 Sept. 2001
20. B.S. Lee, A.R. Nix and J.P. McGeehan, "Indoor space-time propagation modelling using a ray launching technique", *IEE International Conference of Propagation Modelling*, April 2000

BIOGRAPHIES

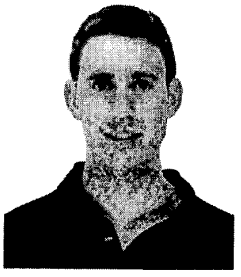

Andrew Lillie received the MEng degree from the University of Bristol in 2000. He is currently studying for a PhD at the University of Bristol. His research interests include, iterative decoding and equalisation techniques for WLAN and WPAN applications.

Andrew Nix received his BEng and PhD degrees from the University of Bristol in 1989 and 1993 respectively. He is currently Professor of Wireless Communication Systems. His main research interests include broadband wireless communications, radiowave propagation modelling, cellular network optimisation and advanced digital modulation/reception techniques. He currently leads the propagation modelling and wireless Local Area Network groups in the Centre for Communications Research (CCR). He has published in excess of 160 Journal and Conference papers and is a member of the IEEE.

Paul Fletcher received MEng and PhD degrees from the University of Newcastle-upon-Tyne (UK) in 1989 and 1993 respectively. He joined the low cost phased array antenna group QinetiQ Ltd. (formerly DERA) in 1993. He is currently a Visiting Research Fellow at the University of Bristol (UK). His research interests encompass mutual coupling compensation techniques, low sidelobe beamforming, adaptive beamforming, space-time signal processing, MIMO and spatial diversity techniques and iterative decoding. He has published over 65 journal and conference papers and holds four patents. He currently leads the space-time processing activities of the array antenna group for next generation wireless LAN and PANs within QinetiQ Ltd. He is a member of the IEE and IEEE.

Joe McGeehan is presently professor of communications engineering and dean of engineering at the University of Bristol. He is also managing director of Toshiba Research Europe Limited: Telecommunications Research Laboratory (Bristol). He has been actively researching spectrum-efficient mobile radio communication systems since 1973, and has pioneered work in many areas, including linear modulation, linearized power amplifiers, smart antennas, propagation modelling/prediction using raytracing, and phase-locked loops. In 1993 he was elected a Fellow of the Royal Academy of Engineering.